UNIVERSITÀ
DEGLI STUDI
FIRENZE
DST
DIPARTIMENTO DI
SCIENZE DELLA TERRA

Emanuele Marchetti
Department of Earth Sciences,
University of Firenze
Via G. La Pira, 4
50121, Firenze
Italy

To the Editor of the
Earth Surface Dynamics

Firenze, February 24, 2020

Dear Editor,

I submit to your attention for publication on Earth Surface Dynamics the manuscript “Seismo-acoustic energy partitioning of a powder snow avalanche”, written in cooperation and agreement with Alec van Herwijnen, Marc Christen, Maria Cristina Silengo and Giula Barfucci. The manuscript was revised following the comments of the two reviewers, Emma Surinach and Bradley Lipovsky.

All the comments of the reviewers have been addressed in the text and we are grateful as they allowed us to greatly improve the manuscript. Below we provide a point-by-point reply to the comments of the reviewers and a version of the manuscript with track changes.

Hoping in your interest in this topic, I thank you in advance for your time.

Sincerely
Emanuele Marchetti

UNIVERSITÀ
DEGLI STUDI
FIRENZE
DST
DIPARTIMENTO DI
SCIENZE DELLA TERRA

**Reply to the review by Bradley Lipovsky**

*Reviewer: I would suggest caution when considering the partitioning of radiated energy between infrasonic and seismic waves for several reasons. The results are somewhat limited by the use of a geophone which is relatively insensitive to low frequencies. I furthermore would generally expect the seismic signal to be lower frequency than the infrasound.*

Unfortunately, the high frequency response of the geophone is a clear limitation. This was correctly pointed out from both reviewers. Therefore, we pointed out such a limitation in the text, wherever it applies, in order to make clear that the results might be partly affected by the geophone frequency response. Definitely, in the future we will have to deploy a broadband seismometer collocated with the infrasound array.

*Reviewer: The simple Equation 1 does not account for the frequency dependence of waves through a porous snow layer and should be taken with a grain of salt. It also does not account for the specific generation of surface waves which the authors later claim to be important.*

Equation 1 describes the transition of infrasound wave (longitudinal waves) to the ground as vertical seismic velocity (body waves). It depends solely from the elastic constant of the medium ($\mu$ and l). This aspect has been clarified in the text.

*Reviewer: I would generally recommend clarifying the distinction between observations and interpretations/results/models. Examples include: First paragraph of Section 4 talks about seismo-acoustic records and their interpretation at the same time. Section 3 (line 104 on) talks about the model. Section 5 largely consists of discussion points. It would improve the readability of the paper to follow a more traditional structure; i.e., Data, Methods, Results, Discussion.*

The paper was re-organized following the suggestion of the reviewer. All the changes are clearly highlighted in the track changes version.

*Reviewer: Figure 6 is in units of counts rather than m/s, which makes it difficult for the reader to asses the scale.*

We changed the scale of the figure into m/s.

*Reviewer: Line 92-93 Two seconds error seems like rather poor timing. Did any of the instruments use GPS for timing?*

The infrasound array is equipped with a GPS receiver for time synchronization (line 89). The seismic array was not, and used a GPS receiver to synchronize the acquisition computer clock. There might be an error here. Therefore, we aligned seismic and infrasound data with the occurrence of local earthquakes that were recorded by both system. Here comes the error of two seconds, that despite being very large considering GPS timing, is very low for the aim of our research, that aims to compare seismic and infrasound data at the timescale of the event (tens of seconds).

UNIVERSITÀ
DEGLI STUDI
FIRENZE
DST
DIPARTIMENTO DI
SCIENZE DELLA TERRA

*Reviewer: Could the observations be related to recent work suggesting a more nuanced avalanche classification system (i.e., Kohler et al., 2018 10.1002/2017JF004375)?*

A reference to the work by Kohler et al., 2018 has been included in the introduction when describing the PSA that basically corresponds to the Intermediate Regime identified by Kohler et al., 2018.

UNIVERSITÀ
DEGLI STUDI
FIRENZE
DST
DIPARTIMENTO DI
SCIENZE DELLA TERRA

**Reply to the review by Emma Surinach**

*Reviewer: It is a very interesting contribution, although the authors have not take into account the previous paper of Kogelnig et al., (2011) where seismic and infrasound time series are compared for four different types of avalanches at the VdLS experimental site, descending along different paths, unlike the one presented in the manuscript under review in which only one avalanche is studied. In this paper the infrasound and seismic time series obtained in collocated sensors with a common time are compared, and also with the time series obtained in two more seismometers placed along the avalanche path. Additionally, a comparison was made with other "in situ" direct measurements (flow depth and internal velocities). The frequencies involved in the study are in the range of [1-40] Hz for both type of measurements. Of interest is the content of "low" [1-3] Hz frequencies of the seismic when comparing with the infrasound. Because of the completeness of these data, with respect to that of the data of the manuscript under review, the authors must take into account in their discussion and conclusions the results obtained previously. In principle, part of the obtained results by the authors could confirm the previous ones or contradict them.*

We are perfectly aware of the work performed by Kogelnig et al., 2011, and it was already referenced in the text. However, following the comment of the reviewer, we included a better discussion of our findings compared to what presented already by Kogelnig et al., 2011.

*Reviewer: The use of the combination of the two arrays in this study is very positive, but the authors must be aware of the limitations of their study. In addition, the results presented also depend on the specific topography. One of the difficulties of the comparison of the results of the two arrays is that the infrasound array has a direct view of the avalanche flow and the array of geophones does not. What would happen in the case of the existence of a shadow zone for the infrasound? Or if the seismic array had been collocated with the infrasound array?*

Infrasound propagation is strongly affected by the local topography. Basically, moving sources that are not line-of-sight to the infrasound array, are recorded with a limited variation of back/azimuth and/or apparent velocity. This is not the case of seismic data, that propagate in the ground, even if, in this case, variable seismic phases can make the analysis more complicated. This aspect has been further discussion in the manuscript. In case of a collocated seismic and infrasound array, p-wave induced variation of back-azimuth would mimic the back-azimuth variation induced by infrasound.

*Reviewer: As regards Section 5. Kogelnig et al. (2011) includes a section dedicated to the source of infrasound and seismic signals. There, a synthetic signal is obtained using the expression of Ffowcs Williams (1963) that describes the acoustic intensity generated by a turbulent source in motion. The modeling results are compared with the infrasound time series obtained from an avalanche. In addition, due to the existence of a suspension layer that can generate infrasound, an explanation is included for not considering a unic specific source of infrasound.*

UNIVERSITÀ
DEGLI STUDI
FIRENZE
DST
DIPARTIMENTO DI
SCIENZE DELLA TERRA

Following the comment of the reviewer, we included a comment this aspect in the discussion of the source mechanism of the infrasound signal.

*Reviewer: In addition, the flow dimension D is calculated for the dominant frequencies. The authors must take into account in their discussion and conclusions the results obtained previously.*

We completely agree with the reviewer. A discussion about this aspect, following the work performed by Kogeling et al., 2011, is included in the manuscript.

*Reviewer: A remark on Figure 4. This figure is very important in the interpretation of the time series and the results. Note that the origin of the time series corresponds to the farthest distances. To facilitate interpretation with the time series, the authors must convert the distances into time (using the obtained speeds) and reverse the origin of the distance. In addition, the slope angle (derived from the profile) incorporated in Figure 4d with the outputs of the RAMMS model will help to better correlate the slope change with the features of the time series.*

We thank the reviewer for this comment and we changed the figure. In particular we reversed the distance and divided the flow depth and flow velocity in two different subplots, and over-imposed that in the path profile, in order to highlight correlation of avalanche parameters and path geometry. Following the comment of the reviewer, we also tried converting distance into time, but found the output figure misleading and of difficult comprehension at this stage of the manuscript, where the recorded infrasound and seismic time series are not introduced yet. The new figure, realized after some of the comments of the reviewer, is definitely much clearer. The figure caption has been chaged accordingly.

*Reviewer: The limitation in the frequency content used in the study must be indicated in the abstract.*

This is now included in the abstract.

*Reviewer: - Line 48. Please, confirm that reference Naugolnykh, K., and Bedard, A is correct. There are different contributions of these authors with the same title, e.g.*

The reference has been double-checked and corrected. The correct reference is:

Naugolnykh, K., and Bedard, A., (2002): A model of the avalanche infrasonic radiation. A IEEE International Geoscience and Remote Sensing Symposium DOI: 10.1109/IGARSS.2002.1025713.

*Reviewer: Lines 76- 90. -Line 77. Please, check the figure numbers. e.g. Is figure 2c correct or it is 1b?*

The reviewer is perfectly right. This was corrected in the text.

*Reviewer: Although it is indicated in the abstract you must mention here the distance between the arrays -Line 85. Figure 1c?*

This information has been added in the text.

*Reviewer: -Lines 91-93. This assertion will be correct assuming that the earthquake is recorded in the infrasound sensors. An explanation on this, references, or more detail is needed. ...*

Seismic ground shaking is routinely recorded on infrasound sensors. The shaking of the ground causes a movement of the infrasound sensor and therefore a variation of pressure. Just to provide an example, the datasheet of mb3 sensor by seismowave provide the seismic sensitivity (http://seismowave.com/medias/documents/MB3a.pdf). We believe that a reference here is probably redundant.

*Reviewer: <2 s assuming the difference in wave travel time and wave propagation speeds of ... and a distance of ... -Line 100. Please, check if Figure 3 is correct.*

Following the comment of the reviewer, more detail is provided in the text.

*Reviewer: - Line 123. Indicate which sensor corresponds to the time series presented in Figures 5 a and b. Or are they stacked time series?*

The time series in Figure 5 a and b correspond to the 3$^{rd}$ sensor of both arrays. We specified that in the figure caption.

*Reviewer: - Line 131. Are you sure about 35 s? Could you specify the signal limits here even if you do it below?*

This value is not correct. The infrasound signal is approximately 45 seconds. We corrected the text.

*Reviewer: - Lines 140-143. In fact, there are two speeds, one of the infrasound waves in the air and the other corresponding to the source (avalanche). Authors should specify this somewhere, here or above in the presentation of the method.*

In the work we never deal with the velocity of the avalanche.

*Reviewer: - Line 147 February*

Corrected in the text.

*Reviewer: - Line 149. Note that the only effect of the low pass filter is in the infrasound, because the geophones natural frequency is 4.5 Hz*

Yes, the reviewer is perfectly right, thanks for the note.

*Reviewer: - Line 160 approx. 35 s as indicated in Line 131.*

This was fixed in the text.

UNIVERSITÀ
DEGLI STUDI
FIRENZE
DST
DIPARTIMENTO DI
SCIENZE DELLA TERRA

*Reviewer: - Line 162. An explanation of the difference between the detection of time arrival of the matrix and that of the seismic amplitudes observed at 18.30 (Figure 5a) that are clearly due to the avalanche is necessary. Given that the velocity of the seismic waves in relation to the avalanche speed and that of the infrasound in the air, it seems that the avalanche started earlier than indicated.*

Around 18:30 we obtain the first clear detection of seismic signal produced by the avalanche. The first detection of infrasound is recorded after, both because it started to be produced after during the flow and because propagation speed of infrasound is lower.

*Reviewer: - Lines 167-169. Does it refer to the processing of the seismic array or that of in- frasound? Please specify. Vilajosana et al. (2007a) obtained the mentioned ground phase velocities from waves generated by explosions at Ryggfonn. These speeds are independent of avalanches. This is a feature of the site. I think there is a misunder- standing. Please clarify.*

Line 167-169 refers to the processing of seismic wave. We clarified that in the text.

*Reviewer: - Line 176. Section 5. See previous comment on this.*

*DONE*

*Reviewer: - Line 181. Auxiliary material. Do you mean the video? Include the reference.*

Yes, this is what we mean. Text was corrected accordingly.

*Reviewer: - Line 181. ..radiated from a point source*

Corrected in the text.

*Reviewer: - Line 184. ... along the path considering a point source*

Corrected in the text.

*Reviewer: - Lines 210-211. This could be an effect of the relative position of the arrays as men- tioned by the authors in Line 214.*

This is a possibility and is discussed in the text.

*Reviewer: - Line 227. With your results, there is not enough information to generalize to all the avalanches, in plural.*

We are quite confident that snow avalanches are characterized by a predominant source of infrasound energy. Based on previous experimental studies this is likely the front. This is very different for example from other density currents such as lahars and debris flows, where array processing identifies a clear lack of coherence that is interpreted as muktiple sources acting at once. This aspect has been clarified in the text.

UNIVERSITÀ
DEGLI STUDI
FIRENZE
DST
DIPARTIMENTO DI
SCIENZE DELLA TERRA

*Reviewer: - Line 232. Remember the content in Kogelnig et al., (2011).*

The study of Kogelnig is discussed in detail. They analyse infrasound in terms of the elastic energy radiated by the turbulent flow at the avalanche front. Results are very promising. In terms of array analysis however, it can be considerd as a point source moving downhill. Therefore we believe that additional comment here, once the point above has been addressed are redundant. Moreover, in Kogeling too a point source is assumed to estimate the size (D) that is eventually used to calculate infrasound energy radiation by the turbulent flow.

*Reviewer: - Line 246. and references therein....*

Corrected in the text

*Reviewer: - Line 249. Note that the effect of filtering from 1 to 10 Hz and realistically, from 4.5 to 10 Hz, also presents problems in the quantification of the energy, since part of the signal is lost.*

Following the suggestion of the reviewer, the frequency limitation of our study has been highlighted clearly in the text.

*Reviewer: - Line 252. This was also mentioned in Kogelnig et al., (2011)*

The reference is added in the text.

*Reviewer: - Line 260-264. The authors must specify that this is in the range of frequencies con- sidered [1-10 Hz] and [ 4.5- 10 Hz], respectively.*

Same as above. This has been stated clearly in the abstract, methodology and conclusions.

*Reviewer: - Line 275. Please specify this reference. See Line 48.*

Reference has been corrected in the text and reference list.

*Reviewer: - Line 277. Are you sure that including Π in eq. 2 is correct? Are you considering radians?*

Yes. Considering a regid sphere that starts moving into the atmosphere, the characteristic angular frequency is proportional to the ratio between the sound wave propagation velocity and the radius of the sphere, resulting into equation 2. This equation, proposed to investigate the frequency of infrasound radiated by a snow avalanche by Naugolnykh, K., and Bedard, A., was developed already by Landau and Liftshitz, (Fluid Mechanics, 1959, page 287). We prefer referencing to the work of Naugolnykh, K., and Bedard, A., that applied the physics to snow avalanches, rather than a basic book of Fluid Mechanics.

*Reviewer: - Lines 288 - Specify in the Conclusions that the results correspond to the case of study, for a powder-snow avalanche recorded at 1000 m from the starting point.*

UNIVERSITÀ
DEGLI STUDI
FIRENZE
DST
DIPARTIMENTO DI
SCIENZE DELLA TERRA

This has been specified in the text.

*Reviewer: - Line 292. ....source mechanism of the infrasound*

Corrected in the text.

*Reviewer: - Line 293. Specify the wave parameters (back-azimuth and apparent velocity) or rephrase the two sentences.*

Corrected in the text.

*Reviewer: - Line 294....purposes in the case that a powder part develops.*

Corrected in the text.

*Reviewer: - Line 295. What happens if there is a sharp change in the slope were a powder part is also developed? See e.g. https://www.youtube.com/watch?v=WAbIcWxwGg4*

According to our findings and experience, infrasound is strongly controlled by the evolution of the powder cloud. Therefore, stable infrasound will be produced at the site where slope changes. Such a behavior was observed also for debris flow (Marchetti et al., 2019, JGR) ad enhanced infrasound is radiated at waterfalls that are detected despite the flow keeps moving downhill.

*Reviewer: - Line 303. Please indicate in % what it means strongly affected. In addition, you must consider the different frequency content of the two time series in your calculations.*

This has been addressed in the text.

*Reviewer: - Line 313. Energy radiation*

This has been corrected in the text.

*Reviewer: - References Please, Indicate correctly the spelling of the surnames.*

Reference list has been doublechecked carefully.

*Reviewer: -Figures - Figure 1. In Figure 1b) the s7 sensor is missed.*

There was s1 twice. This was corrected in the figure.

*Reviewer: Figure Caption 1. Replace "array" by (c) arrays. Indicate the meaning of si and mi.*

Figure caption was corrected. s1-s7 are seismometers 1-7 and m1-m5 are microphones 1-5.We think that specifying that is probably redundant.

UNIVERSITÀ
DEGLI STUDI
FIRENZE
DST
DIPARTIMENTO DI
SCIENZE DELLA TERRA

*Reviewer: - Figure Caption 2. Replace runout zone by maximum runout zone.*

Figure caption has been corrected.

*Reviewer: - Figure Caption 3 Specify the array (infrasound?). The arrays are distant 500 m and the scale is not included.*

Figure caption has been corrected.

*Reviewer: - Figure 4. Redraw figures c) and d) according to my previous comments*

Subplots c and d have been replaced.

*Reviewer: - Figure 5c) Replace spectal by spectral.*

Figure has been corrected.

*Reviewer: - Figure 6. In Figure 6b) convert counts to ground speed and include in the horizontal axis the title like Figure 5a. For the benefit of the comparison, change the vertical scale on a more detailed scale for the posterior azimuth 6d) and the apparent velocity 6f) of the seismic data, even if you lose some outliers.*

Figure 6 has been modified following all the suggestions of the reviewer.

*Reviewer: - Figure 7. Indicate units, when necessary, in the Figure and in the Figure caption. °N is it correct in Figure 7c).*

Figure 7 has been corrected according to the comment of the reviewer.

*Reviewer: - Figure Caption 8. Indicate the location of the arrays. C6*

The figure caption has been corrected following the comment of the reviewer.

# Seismo-acoustic energy partitioning of a powder snow avalanche

Emanuele Marchetti[1], Alec van Herwijnen[2], Marc Christen[2], Maria Cristina Silengo[1], and Giulia Barfucci[1]

[1]Department of Earth Sciences, University of Firenze, Firenze, Italy.
[2]WSL Institute for Snow and Avalanche Research SLF, Davos, Switzerland.

**Correspondence:** Emanuele Marchetti (emanuele.marchetti@unifi.it)

**Abstract.** While flowing downhill, a snow avalanche radiates seismic waves in the ground and infrasonic waves in the atmosphere. Seismic energy is radiated by the dense basal layer flowing above the ground, while infrasound energy is likely radiated by the powder front. However, the mutual energy partitioning is not fully understood. We present infrasonic and seismic array data of a powder snow avalanche, that released on 5 February 2016, in the Dischma valley above Davos, Switzerland. A five element infrasound array, sensitive above 0.1 Hz, and a seven element seismic array, sensitive above 4.5 Hz, were deployed at short distance ($<$ 500 m) from each other, and close ($<$ 1500 m) to the avalanche path. The avalanche dynamics was modeled by using RAMMS, and characterized in terms of front velocity and flow height. The use of arrays rather than single sensors, allowed us to increase the signal-to-noise ratio, and to identify the event in terms of back-azimuth and apparent velocity of the recorded wave-fields. Wave parameters, derived from array processing, were used to identify the avalanche path and highlight the areas, along the path, where seismic and infrasound energy radiation occurred. The analysis showed that seismic energy is radiated all along the avalanche path, from the initiation to the deposition area, while infrasound is radiated only from a limited sector, where the flow is accelerated and the powder cloud develops. Recorded seismic signal is characterized by scattered back-azimuth, suggesting that seismic energy is likely radiated by multiple sources acting at once. On the contrary, infrasound signal is characterized by a clear variation of back-azimuth and apparent velocity. This indicates that infrasound energy radiation is dominated by a moving point source, likely consistent with the powder cloud. Thanks to such clear wave parameters, infrasound revealed particularly efficient for avalanche detection and path identification. While the infrasound apparent velocity decreases as the flow moves downhill, the seismic apparent velocity is quite scattered, but it lowers down to sound velocity during the phase of maximum infrasound radiation. This indicates an efficient process of infrasound to seismic energy transition, that, in our case, increases $\approx$ 20 % the recorded seismic amplitude, at least in our frequency band of analysis of the seismic data. Such an effect can be accounted for when avalanche magnitude is estimated from seismic amplitude. Presented results clearly indicate how the process of seismo-acoustic energy radiation by a powder avalanche is very complex, and likely controlled by the powder cloud formation and dynamics, and is hence affected by the path geometry and snow characteristics.

## 1 Introduction

As a first approximation, powder snow avalanches (PSA) can be described with a two layer model consisting of a dense basal snow layer, with densities of 100-400 kg/m$^3$, and a powder part that develops at the head of the flow, with density of 3-30 kg/m$^3$ (*Issler*, 2003). PSA corresponds to the intermittent regime (IR) identified from GEORADAR analysis at the Vallée del la Sionne test site by *Kohler et al.* (2018) that are characterized by intense surging activity, flow heights up to 9 m, front velocity up to 60 m/s and develop once snow temperature is always < -2 degrees C. *Carrol et al.* (2013) provided a detailed analytical description of the powder front of a PSA in terms of an eruption current. They showed how the front evolution is mostly controlled by the amount of snow scoured from the snowpack, as the front moves downhill. This erosion depends on the characteristics of the snowpack, such as density and temperature, and channel morphology (see e.g. *Louge et al.*, 2012; *Carrol et al.*, 2013). The formation of the powder front is enhanced by the narrowing of the avalanche channel, while the front spreading causes deceleration and consequent collapse of the front. Moreover, *Steinkogler et al.* (2014) showed how the evolution of the powder cloud is affected by the temperature of the snow cover. They showed that the temperature of - 2 degrees C of the scoured snow, is a threshold value between different dynamics, with the cloud formation inhibited for "warm avalanches".

While flowing downhill, the interaction of the dense basal flow with the ground radiates seismic energy (*Sabot et al.*, 1998). Infrasound energy is radiated by the compression of the atmosphere produced mostly by the powder front (see e.g. *Schaerer and Salway*, 1980; *Bedard*, 1989). The ratio between the dense and powder part of a snow avalanche, and hence between the seismic and infrasound energy radiation, is not constant while it depends on the front evolution through time (*Carrol et al.*, 2013).

Seismic measurements have been widely applied to investigate avalanche dynamics and characteristics. *Sabot et al.* (1998) showed that slope changes, and the presence of obstacles on the flow path strongly affect the radiation of seismic energy. Moreover, characteristics of recorded seismic signals depend on snow density and avalanche type and size (*Biescas et al.*, 2003; *van Herwijnen and Schweizer*, 2011b; *Vilajosana et al.*, 2007b). Seismic monitoring techniques deploying multiple sensors along the avalanche path (*Biescas et al.*, 2003; *Vilajosana et al.*, 2007a) or arrays (*van Herwijnen and Schweizer*, 2011a; *Lacroix et al.*, 2012; *Heck et al.*, 2017), that allow to identify the avalanche occurrence within a source-to-receiver distance up to $\approx$ 3 km. *Hammer et al.* (2017) recorded very large avalanches up to 30 km away.

After the pioneer study by *Bedard* (1989), the use of the infrasound in avalanche monitoring and research has increased significantly (*Chritin et al.*, 1996; *Adam et al.*, 1998; *Comey and Mendenhall*, 2004). *Naugolnykh and Bedard* (1990) suggested that infrasound is possibly induced by the non-stationary motion and/or by the turbulence of the flow. Moreover, they suggested that the amplitude and frequency of the recorded infrasound signals should scale with the avalanche size and velocity.

Since then, infrasound avalanche observations improved substantially, both in number and accuracy. The development and use of infrasound arrays instead of single sensors (*Scott et al.*, 2007; *Ulivieri et al.*, 2011; *Havens et al.*, 2014; *Marchetti et al.*, 2015), allowed to increase the signal-to-noise ratio and to improve the investigation of the avalanche infrasound signature. Specific wave parameters (back-azimuth and apparent velocity) of recorded signals were used to define array processing pro-

cedures, able to detect medium size snow avalanches at distances of a few kilometers (*Ulivieri et al.*, 2011; *Marchetti et al.*, 2015; *Mayer et al.*, 2018). Moreover, infrasound array derived information were used to remotely evaluate the avalanche front position and velocity through time (*Marchetti et al.*, 2015; *Havens et al.*, 2014).

While geophysical observations of snow avalanches significantly improved the monitoring techniques, a robust conceptual model of seismic and infrasound energy radiation is still missing. Previous studies based on infrasound and seismic records allowed to investigate to some extent the mutual characteristics (*Surinach et al.*, 2001; *Kogelnig et al.*, 2011). Kogelnig et al. (2011) , in particular, analyzed 4 avalanches at the Vallée de la Sionne test site that were recorded with infrasound and seismic sensors, and showed that infrasound and seismic energy was produced by the different regimes and their amplitude were roughly correlated to the aerosol and dense layer, respectively. Moreover, they modeled the infrasound energy radiation in terms of a moving turbulent sound source, being the infrasound amplitude proportional to the flow speed and height of the powder cloud. However, many open questions remain and using infrasound and seismic signals to infer avalanche size is still debated. It is well known that seismic and infrasound energy interact at the earth free surface and are transmitted between the atmosphere and solid earth (*Ichihara et al.*, 2012). The transmission affects the amplitude of recorded signal and should be considered when signal characteristics are used to constrain the source process or to calculate the energy of the event.

In this work we present a combined seismic and infrasound array analysis for a snow slab avalanche that occurred on 5 February 2016, in the Dischma Valley, south of Davos, Switzerland. The event was recorded by a seismic and an infrasound array located nearby (less than 1500 m) the path. The data obtained from the seismic and the infrasound array are used to investigate the mutual energy radiation as a function of the front position along the avalanche path. To investigate the properties of recorded signals as a function of event characteristics, the avalanche was modeled using the avalanche simulation software RAMMS (*Christen et al.*, 2010) .

## 2 Study site, instrumentation and data

During the winter of 2015-2016 a seismic ~~array~~ and an infrasound array were colocated, at short distance ($< 500$ m) from each other, in the Dischma valley, south of Davos, in the Eastern Swiss Alps (Figure 1). The installation site is a flat area, at an elevation of $\approx 2000$ m a.s.l. surrounded by peaks rising up to $\approx 3000$ m. On Feb. 5, 2016, a snow slab avalanche released from Chlein Sattelhorn, and was recorded both by the seismic and ~~by~~ the infrasound array (Figure 1, Figure 2a).

The seismic array (Seismic Instruments Inc.) consisted of 7 elements deployed with a circular geometry and maximum aperture (maximum distance between 2 array elements) of 75 m (Figure ~~2c~~1b). The array was equipped with vertical geophones with a corner frequency of 4.5 Hz and a sensitivity of 28.8 V/m/s. The geophones were attached with anchors to large rocks on the ground and subsequently buried by snow, which substantially reduced the effect of wind noise. Seismic data were sampled at each geophone at 500 Hz and 24 bits precision. Data were recorded locally at the central acquisition system. The entire system was powered with solar panels and batteries, and the total power requirement was approximately 7 W.

The infrasound array (FIBRA; www.item-geophysics.it) operated with fiber optic connection among the 5 different array elements. The fiber optic connection allows to increase significantly the signal to noise ratio, and prevents the risk of damage

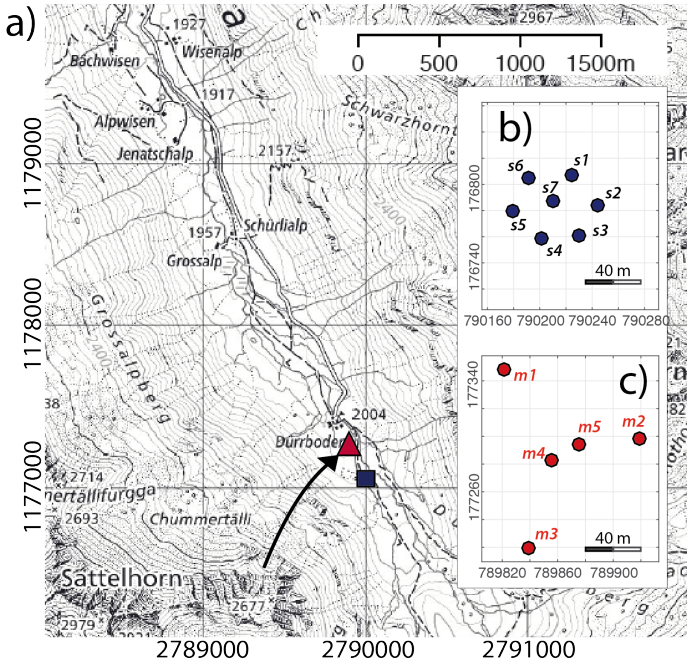


**Figure 1.** Map (a) showing the location of the Dischma valley, south of Davos, Switzerland. The location of the infrasound array (red triangle) and the seismic array (white square) are show, as well as the Chlein Sattelhorn avalanche path (black arrow). Positions are given in Swiss coordinates (CH1903). Reproduced by permission of swisstopo (JA100118). Details of the geometry of the seismic (b) and infrasound ~~array~~ arrays (c).

related to lightning or electric discharges. The array was deployed following a triangular geometry, with two central elements, and had a maximum aperture of 160 m (Figure ~~2d~~1c). Each array element was equipped with a differential pressure transducer (prs025a), with a sensitivity of 400 mV/Pa in the pressure range of +/- 12.5 Pa, and a frequency response between 0.01 and 200 Hz. Analogue pressure data were converted to digital signals at each array element, with a sampling rate of 50 Hz and 16 bits dynamics, and were transmitted trough fiber optic to a central unit, where data were synchronized with GPS timing. ~~Data were both recorded locally and made available trough TCP/IP for data transmission.~~ Power requirement was ≈1 W for the central unit and as low as ≈0.1 W for the array element.

The data recorded by the two arrays were synchronized by comparing the timing of local and regional earthquakes recorded by the infrasound as well as the seismic array. ~~This~~ Considering a propagation velocity $<$ 2000 m/s and a distance of $<$ 500 m between the two arrays, such an approach guarantees a timing accuracy of $<$ 2 seconds, which is sufficient for the seismo-acoustic comparison presented here.

The study site was also equipped with automatic cameras collecting images every ten minutes, used to visually monitor the activity on the slopes surrounding the arrays. The camera system was colocated with the central element of the infrasound array.

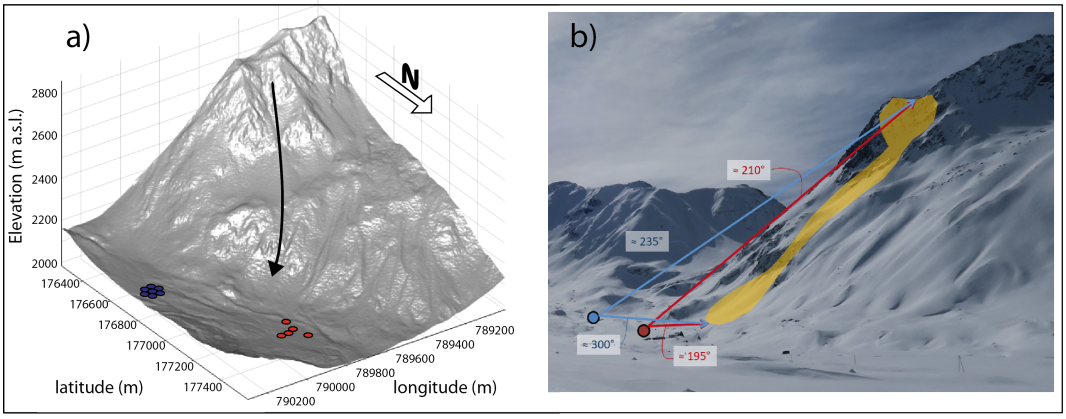


**Figure 2.** (a) Digital Elevation Model showing the installation site within the Dischma valley, south of Davos, Switzerland, with the position of the seismic array (blue dots), the infrasound array (red dots) and the Chlein Sattelhorn avalanche path (black arrow). (b) Photo of the field site with the position of the seismic array (blue dot), the infrasound array (red dot) and the approximate contour of the Chlein Sattelhorn avalanche from 5 February 2016 (orange). The approximate backazimuth angles to the start zone and maximum runout zone of the avalanche relative to the seismic and infrasound array are also shown (colored arrows).

## 3 ~~The dry-snow avalanche of 5 February 2016~~

In the morning of 5 February 2016, at 05:18 UT, a medium sized dry-snow avalanche released from Chlein Sattelhorn (Figure 2b), at an elevation of ≈ 2600 m. The avalanche traveled a distance of 1200 meters and stopped at the bottom of the Dischma valley, at an elevation of ≈ 2030 m at a short distance (<100 m) from the infrasound array (Figure 3). The event occurred during a snow storm. Nevertheless, based on the images from the automatic cameras we confirmed that the avalanche released between 4 February 2016 at 17:40 UT and 6 February 2016 at 07:40 UT. The avalanche deposit was first clearly visible on the morning of Feb. 6 (08:30 UT), when the weather ~~weather~~ cleared (Figure 3~~).~~

~~The flow characteristics and evolution (flow depth and velocity) were reconstructed using the RAMMS model (Figure 8) (*Christen et al.*, 2010). We used RAMMS::Avalanche (version 1.7.20) for the simulations of Chlein Sattelhorn. The model requires a detailed digital elevation model as well as an estimate of the initial release volume, i.e. an initial release area and a fracture depth. The inital digital elevation model (DEM) is the swissAlti3D DEM (2 m grid resolution). For the simulation, we did a bilinear interpolation to 5 m. The release volume (with release depth of 80 cm) was 9.525 $m^3$. We used calibrated friction values for small avalanches, with a return period of 10 years. The modeled flow depth evolution (*Marchetti et al.*, 2020) , predicts a total flow duration of ≈ 90 seconds, with ≈ 60 seconds required by the avalanche to initiate, accelerate, and reach the valley bottom, followed by ≈ 30 seconds of snow deposition. Since the path geometry is characterized by a sharp terrain break at an elevation of approximately 2300 m (Figure 8c), the modeled avalanche accelerated along the release area with slopes exceeding 35 degrees, rapidly decelerated and lost mass at the terrain break (Figure 8d). The modeled avalanche then accelerated again after entering a steep (slope > 30 degrees), narrow channel (< 50 m), within the lowest part of the~~

~~path. Finally, the flow slowed down when it reached the valley bottom at an elevation of ≈ 2030 m (Figures 2,8), where the snow mass was spread out horizontally on the runout area. The modeled snow avalanche qualitatively compared well to the~~
125 ~~information we obtained from the images from the automatic cameras (Figure 2~~b).

~~RAMMS predicted a maximum flow depth of almost 3.5 m, that was reached after a travel distance of ≈ 200 m along the path. The maximum front velocity, of ≈ 35 m/s, was reached at the end of the first, and highest, part of the path, before the deceleration at the terrain break (Figure 8). Lower values of front velocity and flow depth result from the model below the terrain break.~~

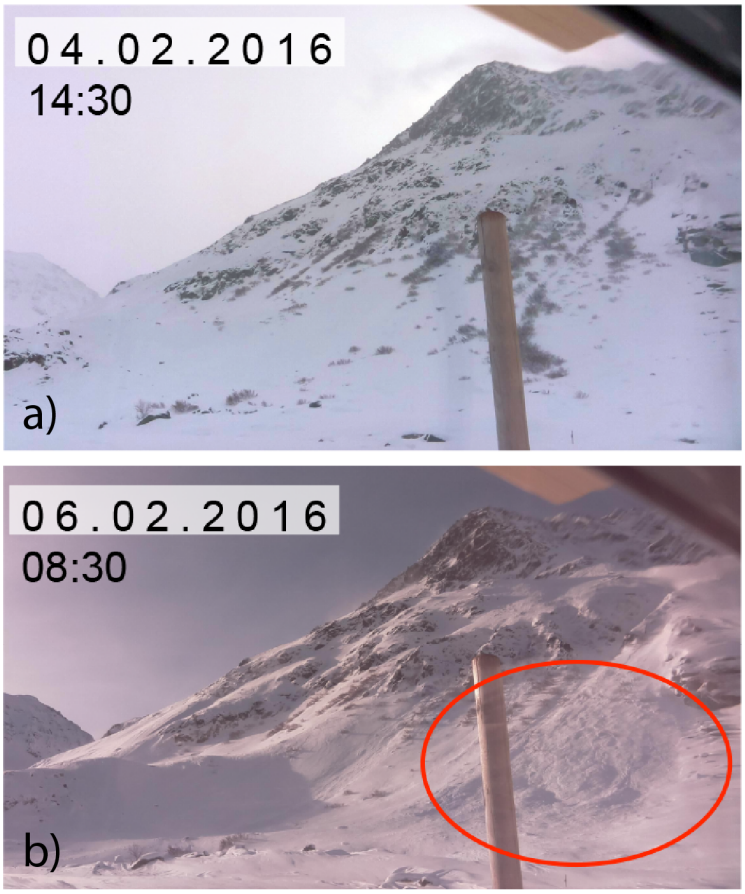


**Figure 3.** Picture showing the slope west from the infrasound array in the afternoon of February, 2nd (a, last clear image before the event) and in the morning of February, 6th, 2016 (b, first clear image after the event) that shows the avalanche accumulation area.

130 ~~Figure showing the flow extent modeled by RAMMS and highlighting maximum flow depth (a) and flow velocity (b). Elevation of the avalanche path (c) as a function of the horizontal distance with respect to the central element of the infrasound array. (d) Profiles of the modeled flow depth (blue) and flow velocity (red) along the path.~~

## 3 ~~Seismo-acoustic records of the event~~

The event from 5 February 2016 was clearly recorded by the seismic and infrasound arrays (Figure 4a, b) (*Marchetti et al.*, 2020). ~~Both signals consisted of two distinct phases, according with the flow evolution modeled by RAMMS (Figure 8). These two phases appear to be controlled by the path geometry forcing the avalanche to slow down and loose mass at the terrain break at an elevation of 2300 m.~~

The seismic signal has an emergent waveform and a duration of $\approx$ 60 s. It is characterized by two phases of similar amplitude (1.5 $10^{-6}$ m/s), peaking around 05:18:50 and 05:19:20 UT. The signal spectrum shows energy mostly confined between 3.5 and 12 Hz, with the peak frequency around 6 Hz. The frequency response of the geophones limits the spectral analysis to frequencies $>$ 4.5 Hz (Figure 4c), therefore we cannot exclude lower frequency components.

The infrasound record of the event is shorter ($\approx$ ~~35~~ 45 sec), has a similar emergent waveform, with two sparate phases reaching a maximum amplitude of $\approx$ 0.5 Pa (Figure 4b). The spectral energy of the infrasound signal is wider, spanning between 0.5 and 8 Hz, with a clear peak at $\approx$ 3.3 Hz (Figure 4c).

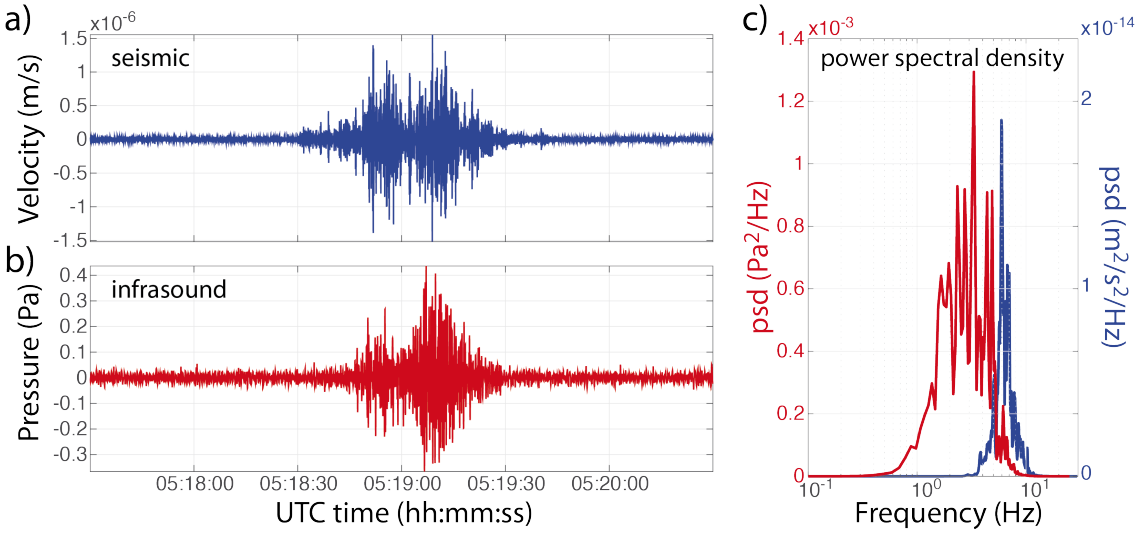


**Figure 4.** Seismic (a) and infrasound (b) ~~record~~ signal of the avalanche that occurred on 05 February ~~2016.~~ 2016 recorded by sensor s3 of the seismic array and by sensor m3 of the infrasound array (Figure 1b, c) . c) Power Spectral Density (psd) of the seismic (blue) and infrasound signal (red).

## 3 Methods

The infrasound and seismic data were processed by applying a multichannel correlation analysis, to identify signal from noise in terms of signal back-azimuth and apparent velocity. The procedure, described in detail by *Ulivieri et al.* (2011), identifies coherent data recorded within a given time window assuming planar wavefront propagation. Once a coherent signal

is identified, based on signal correlation threhsold ($> 70$ %), the corresponding back-azimuth ($Baz$) is calculated. The back-azimuth corresponds to the propagation angle from the array to the source, measured with respect to the geographic North in the horizontal plane of the array. Once the back-azimuth is identified, the apparent velocity ($c_a$) is calculated, as the ratio between the real propagation velocity ($c$) and the sin of the take off angle ($c_a = c/\sin\theta$). The apparent velocity corresponds to the velocity the wave would have if it was traveling in the plane of the array, and increases for higher elevation sources. It would be infinite for a source located directly above the array, as all the elements of the array would record the signal simultaneously.

In the specific case of snow avalanches, i.e. a source moving downhill, the apparent velocity is expected to decrease with time (*Marchetti et al.*, 2015). Similarly, ~~the~~ depending on the movement of the avalanche relative to the array, the back-azimuth is expected to change with time. This aspect has been used to identify snow avalanches from other sources with infrasound array analysis, allowing for real-time monitoring and identification of snow avalanches at source-to-receiver distances of several km (*Marchetti et al.*, 2015; *Ulivieri et al.*, 2011; *Mayer et al.*, 2018).

~~For the avalanche from~~ Following the approach described by *Marchetti et al.* (2015), we use the back-azimuth and the apparent velocity of the seismic and the infrasound detections to investigate the position along the avalanche path considering a point source, where the different portions of the signals are generated. For each point of the DEM, we calculate the corresponding values of back-azimuth from the seismic ($Baz_s$) and infrasound ($Baz_i$) arrays, and the expected values of apparent velocity ($c_a$) of the recorded infrasound wavefield (Figure 5). We obtain a map of theoretical values, showing the expected values for the seismic and infrasound wave parameters produced by any point source located on the DEM. A point source moving along any path on the topography would therefore be recorded with values of back-azimuth and apparent velocity, varying according to the theoretical values.

The back-azimuth provides an estimate of the source position in the horizontal plane defined by the array, while apparent velocity is reflecting the source elevation. As expected, the map shows that the back-azimuth varies between 0 and 360 degrees around the seismic and infrasound arrays (Figure 5a, b), independently of the elevation and the distance from the array. The infrasound apparent velocity changes, according to the local topography, from a minimum of 330 m/s up to a maximum value of 400 m/s (Figure 5c), solely affected by the distance from the array and the absolute elevation. Therefore, a proxy of the 3d source position requires combining back-azimuth and apparent velocity. We account simultaneously for back-azimuth and apparent velocity by calculating for each point of the DEM the product ($BV$ = $Baz_i$ x $c_a$) of theoretical values (Figure 5d). The resulting parameter defines a new map, with values depending from both the planar position and source elevation. Such an approach can be easily applied to infrasound wave parameters, while the use of the apparent velocity derived for the seismic wavefield appears complicated by variable phases and complex source-to-receiver travel paths.

In order to correlate the infrasound and seismic wave parameters with avalanche flow characteristics and evolution (flow depth and velocity), we performed flow modeling by using RAMMS (Figure 8) (*Christen et al.*, 2010). We used RAMMS::Avalanche (version 1.7.20) for the simulations of Chlein Sattelhorn. The model requires a detailed digital elevation model as well as an estimate of the initial release volume, i.e. an initial release area and a fracture depth. The initial digital elevation model (DEM) is the swissAlti3D DEM (2 m grid resolution). For the simulation, we did a bilinear interpolation to 5 ~~Ferbruary~~ m. We used calibrated friction values for small avalanches, with a return period of 10 years.

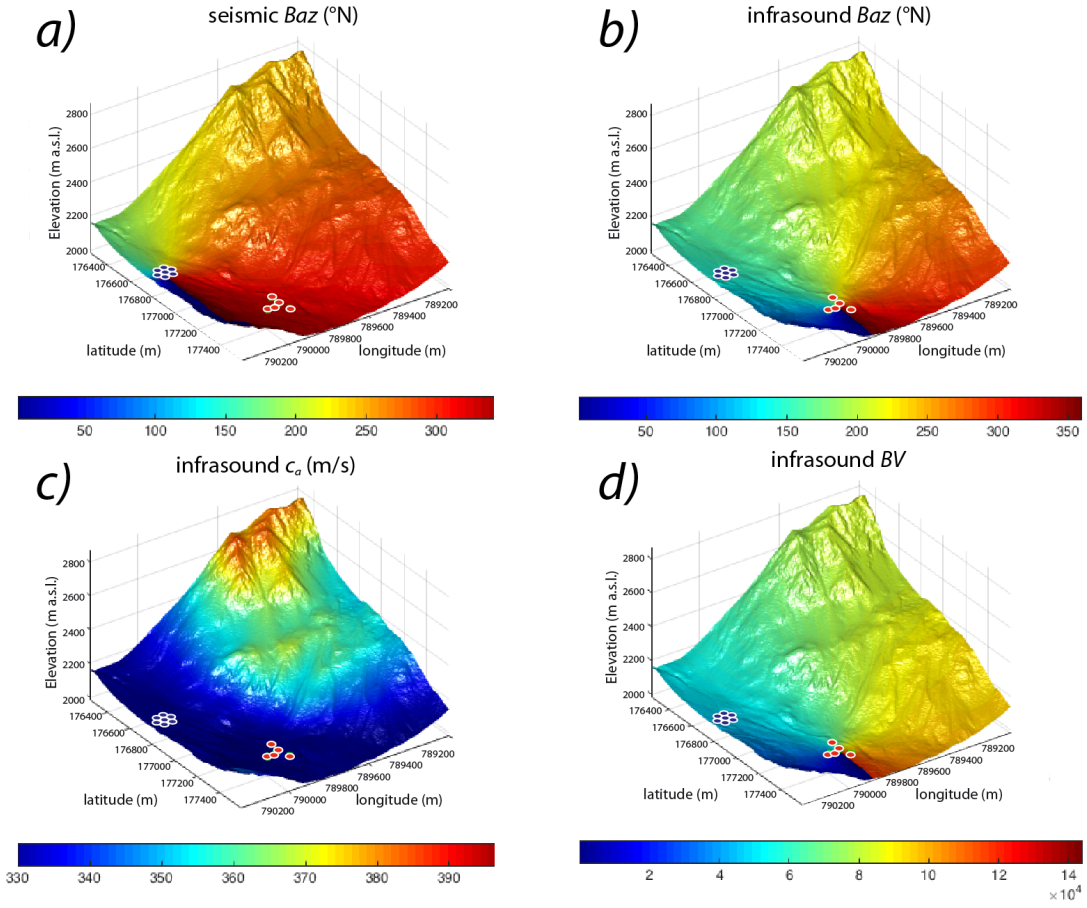


**Figure 5.** Theoretical values of back-azimuth at the seismic array ($Baz_s$ (degrees N), a), back-azimuth ($Baz_i$ (degrees N), b) and apparent velocity ($c_a$ (m/s), c) at the infrasound array for any point source of seismic and infrasound energy located on the DEM. Product between back-azimuth and apparent velocity of infrasound wavefield ($BV$, d). The position of the infrasound and seismic arrays are shown by red and blue circles respectively.

## 4 Results

For the avalanche recorded on 5 February 2016, the multichannel correlation analysis was performed over time windows of 5 seconds, and with an overlap of 4.5 seconds, both for the seismic and for the infrasound data. According to the recorded frequency spectrum (Figure 4c), infrasound and seismic data were bandpass filtered between 1 and 10 Hz. The event then appears as a cluster of detections (Figure 6), each associated with a corresponding value of back-azimuth ($Baz$) and apparent velocity ($c_a$), calculated for each signal time window. From Figure 6, it is clear how infrasound signal starts to be detected at 05:18:50 UTC, with a back-azimuth of 211 degrees N and an apparent velocity of 365 m/s. The apparent velocity decreases

constantly down to 327 m/s, until 05:19:15, while the back-azimuth remains quite stable for the first 15 seconds of the recorded signal, until 05:19:05, and decreases down to 200 degrees N afterwards. Such a variation of apparent velocity and back-azimuth is consistent with the path followed by the observed event, that moves initially North/North-West towards the array (20 degrees N, back-azimuth from the array 210 degrees N), to turn clockwise along the path when the flow moves downhill and approaches the array (Figure 3). Between 05:19:15 and 05:19:25 UTC, the back-azimuth is quite stable, while the apparent velocity increases up to ≈ 350 m/s. We interpret this variation as an artifact, resulting from the short distance between the accumulation area and the array (< 200 m), thereby violating the planar wavefront assumption.

Unlike infrasound, that has a duration of ~~35~~ ≈ 45 seconds and is marked by a clear variation of wave parameters (back-azimuth and apparent velocity), the seismic signal radiated by the event is much longer in duration (≈ 60 sec), and changes in wave parameters were less clear. The first seismic detections were recorded around 05:18:40, ≈ 10 seconds before the first infrasound detection, with a back-azimuth values between 220 and 250 degrees, corresponding reasonably well with the release area of the snow avalanches (Figure 1). During the following 20 seconds we observe a general migration of the seismic back-azimuth, up to ≈ 270-300 degrees N at 05:19:00 UT, corresponding to the runout area. Afterwards, the seismic back-azimuth remains rather stable until the end of the event at 05:19:45 UT.

~~Considering the apparent velocity, the array processing highlights high values (> 650 m/s) at the beginning and at the end of the event. These values are in agreement with phase velocities (500-950 m/s) measured by *Vilajosana et al.* (2007a) for snow avalanches in Ryggfonn in Norway, as well as values used by *Lacroix et al.* (2012) for beamforming in the French Alps. The central part of the signal, between 05:19:00 and 05:19:15 UT, is characterized by a lower propagation velocity (≈ 330 m/s), suggesting that the seismic array is likely recording infrasound waves. This corresponds to the time when the infrasound amplitude was maximum (Figure 6a). We suggest that the central part of the signal is strongly affected by the infrasound radiated by the event, that converts to seismic waves at the earth free surface and is efficiently recorded by seismometers. This is an agreement with results obtained by *Heck et al.* (2017) for an avalanche that did occur from the same path in 2017, and applying the multiple signal classification (MUSIC) analysis to seismic array data.~~

## 5 ~~Elastic energy radiation along the avalanche path~~

The results of infrasound and seismic array processing presented in Figure 6, allow us to describe the mutual infrasound and seismic energy radiation during the avalanche. Just considering the event duration, it is clear from Figure 6, that the avalanche initiation phase is radiating seismic energy in the ground, while no or minor infrasound is radiated into the atmosphere. This is likely related to the first stage of the event, whilst the powder front is not developed yet. Only 20-25 seconds after the avalanche onset, once the flow accelerates ~~(see auxiliary material), infrasound is radiated from~~ (*Marchetti et al.*, 2020), infrasound starts to be radiated by a source that is moving downhill along the avalanche path, as tracked by the infrasound wave parameters (back-azimuth and apparent velocity, Figure 6c, e).

~~Following the approach described by *Marchetti et al.* (2015), we use the back-azimuth and the apparent velocity of the seismic and the infrasound detections to investigate the position along the~~ In order to calculate the portion of the avalanche

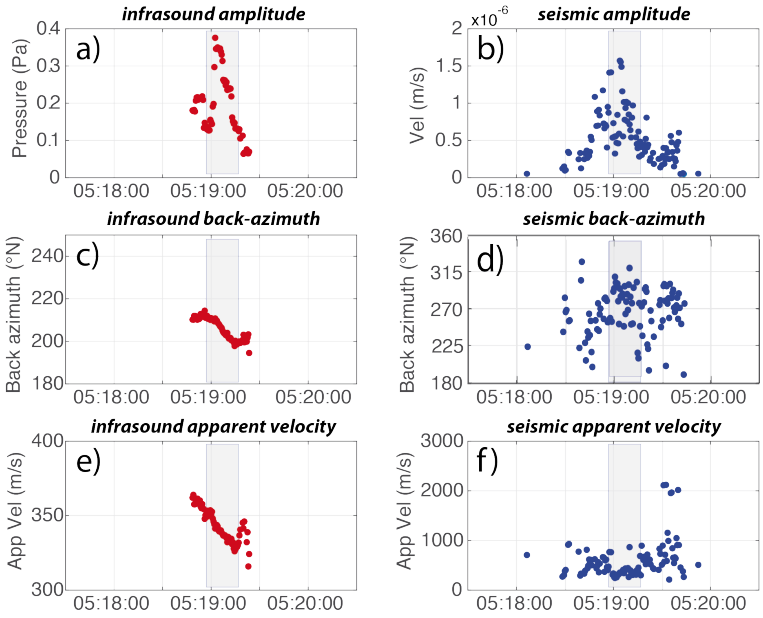


**Figure 6.** Amplitude, back-azimuth and apparent velocity of infrasound (a,c and e, respectively) and seismic (b,d and f, respectively) detections for the avalanche of 5 February 2016. The shaded area highlights the time window of sound propagation velocity recorded for the seismic signal.

path where ~~the different portions of the signals are generated. For each point of the DEM, we calculate the corresponding values of back-azimuth from the seismic ($Baz_s$) and infrasound ($Baz_i$) arrays, and the expected values of apparent velocity ($c_a$) of the recorded infrasound wavefield (Figure 5). We obtain a map of theoretical values, showing the expected values for the seismic and infrasound wave parameters produced by any point source located on the DEM. A point source moving along any path on the topography would therefore be recorded with values of back-azimuth and apparent velocity, varying according to the theoretical values.~~

~~The back-azimuth provides an estimate of the source position in the horizontal plane defined by the array, while apparent velocity is reflecting the source elevation. As expected, the map shows that the back-azimuth varies between 0~~ seismic and ~~360 degrees around the seismic and infrasound arrays (Figure 5a, b), independently of the elevation and the distance from the array. The infrasound apparent velocity changes, according to the local topography, from a minimum of 330 m/s up to a maximum value of 400 m/s (Figure 5c), solely affected by the distance from the array and the absolute elevation. Therefore, a proxy of the 3d source position requires combining back-azimuth and apparent velocity. We account simultaneously for back-azimuth and apparent velocity by calculating for each point of the DEM the product ($BV = Baz_i$ x $c_a$) of theoretical values (Figure 5d). The resulting parameter defines a new map, with values depending from both the planar position and source elevation. Such an approach can be easily applied to infrasound wave parameters, while the use of the apparent velocity derived for the seismic wavefield appears complicated by variable phases and complex source-to-receiver travel paths.~~

Theoretical values of back-azimuth at the seismic array ($Baz_s$, a), back-azimuth ($Baz_i$, b) and apparent velocity ($c_a$, c) at the infrasound array for any point source of seismic and infrasound energy located on the DEM. Product between back-azimuth and apparent velocity of infrasound wavefield (d). The position of the infrasound and seismic arrays are shown by red and blue circles respectively.

Once the theoretical values of the seismic ($Baz_s$) and the infrasound ($Baz_i$) back-azimuth, the infrasound apparent velocity ($c_a$) and their product ($BV$) are evaluated (Figure 5), the source radiating areas for the seismic and infrasound signals can be evaluated from real detections (Figure 6.) We infrasound energies are radiated, we performed a blind search to minimize the difference between wave parameters ($Baz_s$, $Baz_i$, $c_a$ and $BV$) calculated for the seismic and infrasound detections (Figure 6) and the theoretical values calculated for the DEM (Figure 5). Figure (7) shows all the possible source points along the DEM based on the seismic back-azimuth (Figure 7a), the infrasound back-azimuth (Figure 7b), the infrasound apparent velocity (Figure 7c) and their product (Figure 7d). The dark-red areas highlighting all the points of the DEM satisfying a minimum difference threshold. Figure 7 shows that, considering only one parameter at once, only a limited information on the source radiation area can be deduced, unless a constraint of the avalanche path is applied. Such an approach, was applied successfully in previous studies that evaluated the avalanche velocity from infrasound detections (*Havens et al.*, 2014; *Marchetti et al.*, 2015), but limits the analysis to a single avalanche path.

Considering the seismic back-azimuth ($Baz_s$, Figure 7a) only, for example, the detections do not provide any constraint on the source position, as they are consistent with many different directions around the array spanning between 200 and 325 degrees N. However, if we assume that the seismic source is confined within the avalanche path (Figure 2a), it appears that the seismic energy is radiated from the detachment point to the depositional area. Moreover, the scattered values of the back-azimuth of the recorded seismic signals, suggest that multiple sources of seismic energy are active at the same time in different sectors of the avalanche path.

The relative position of the avalanche path and the infrasound array, almost in line, influences the efficiency of the infrasound back-azimuth to identify the source position along the path. Considering the infrasound back-azimuth alone ($Baz_i$, Figure 7b), the back-projection of infrasound detections to the topography does no allow us to constrain the position of the source along the path. The infrasound apparent velocity constrains the source elevation ($c_a$, Figure 7c). The maximum value of the apparent velocity of 364 m/s (Figure 6) limits the energy radiation to the lowest part of the avalanche path, clearly suggesting that no, or minor, infrasound is produced high up in the path during the initiation phase. This conclusion is confirmed by the blind search of the infrasound energy radiation area, based on the combination of back-azimuth and apparent velocity ($BV$, Figure 7d). Here, the minimization of residuals between theoretical and measured values, highlights a limited area on the entire DEM, from the base of the starting zone, where the avalanche accelerates and follows the channel down to the valley.

The clear variation of Position of the back-azimuth and apparent velocity of seismic array is shown by blue circles, while the recorded infrasound signals also provides a strong constraint on the source mechanism of infrasound energy. As discussed in detail by in case of multiple sources,one of the array analysis identifies the most energetic source. Therefore, our results suggest that snow avalanches are characterized by a dominant source of infrasound energy, likely the powder front , allowing to treat the source mechanism of infrasound The location of infrasound and seismic energy radiation along the avalanche path presented

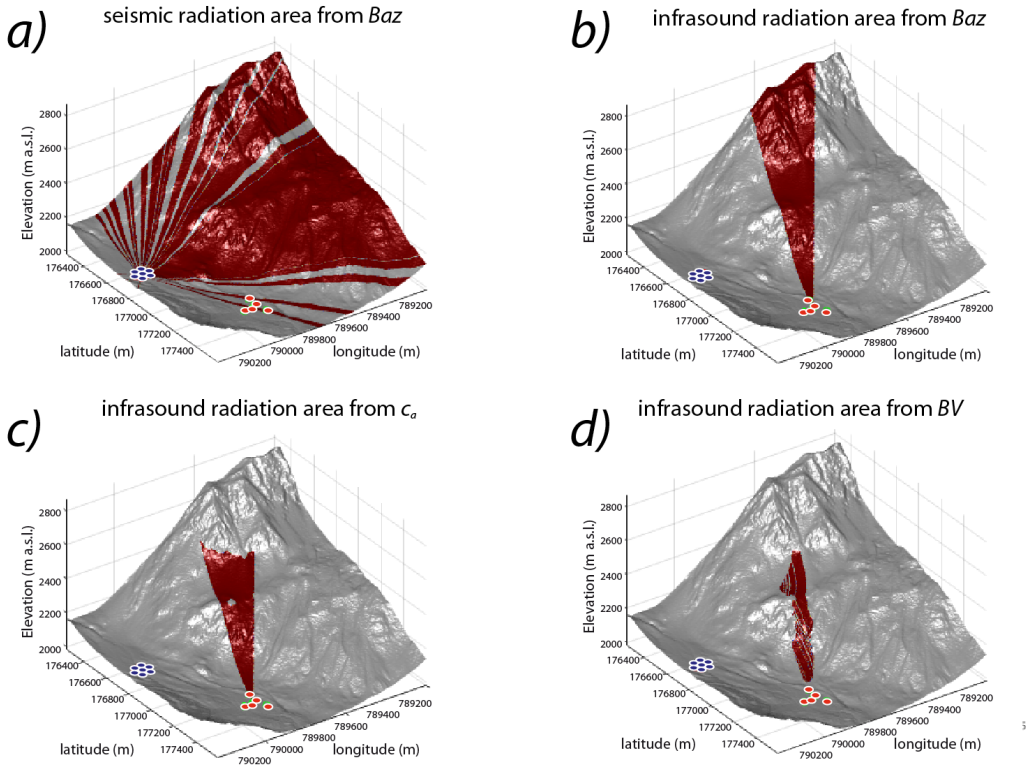


**Figure 7.** Possible radiation areas (dark red) of seismic and infrasound energy, obtained from seismic back-azimuth ($Baz_s$, a), infrasound back-azimuth ($Baz_i$, b), apparent velocity ($c_a$, c) and the combination of infrasound back-azimuth and apparent velocity ($BV$, d)

.

~~in this study,~~ array is In order to investigate the recorded seismic and infrasound signals in terms of avalanche dynamics, we performed RAMMS modeling of the flow evolution (Figure 8). We assumed a release volume of 9.525 $m^3$, with release depth of 80 cm. The modeled flow depth evolution, predicts a total flow duration of ≈ 90 seconds, with ≈ 60 seconds required by the avalanche to initiate, accelerate, and reach the valley bottom, followed by ≈ 30 seconds of snow deposition.

Since the path geometry is characterized by a sharp terrain break at an elevation of approximately 2300 m (Figure 8c), the modeled avalanche accelerated along the release area with slopes exceeding 35 degrees, rapidly decelerated and lost mass at the terrain break (Figure 8d). The modeled avalanche then accelerated again after entering a steep (slope > 30 degrees), narrow channel (< 50 m), within the lowest part of the path. Finally, the flow slowed down when it reached the valley bottom at an elevation of ≈ 2030 m (Figures 2,8), where the snow mass was spread out horizontally on the runout area. RAMMS predicted a maximum flow depth of almost 3.5 m, that was reached after a travel distance of ≈ 200 m along the path. The maximum front

285 velocity, of ≈ 35 m/s, was reached at the end of the first, and highest, part of the path, before the deceleration at the terrain break (Figure 8). Lower values of front velocity and flow depth result from the model below the terrain break. The modeled snow avalanche qualitatively compared well to the information we obtained from the images from the automatic cameras (Figure 2b).

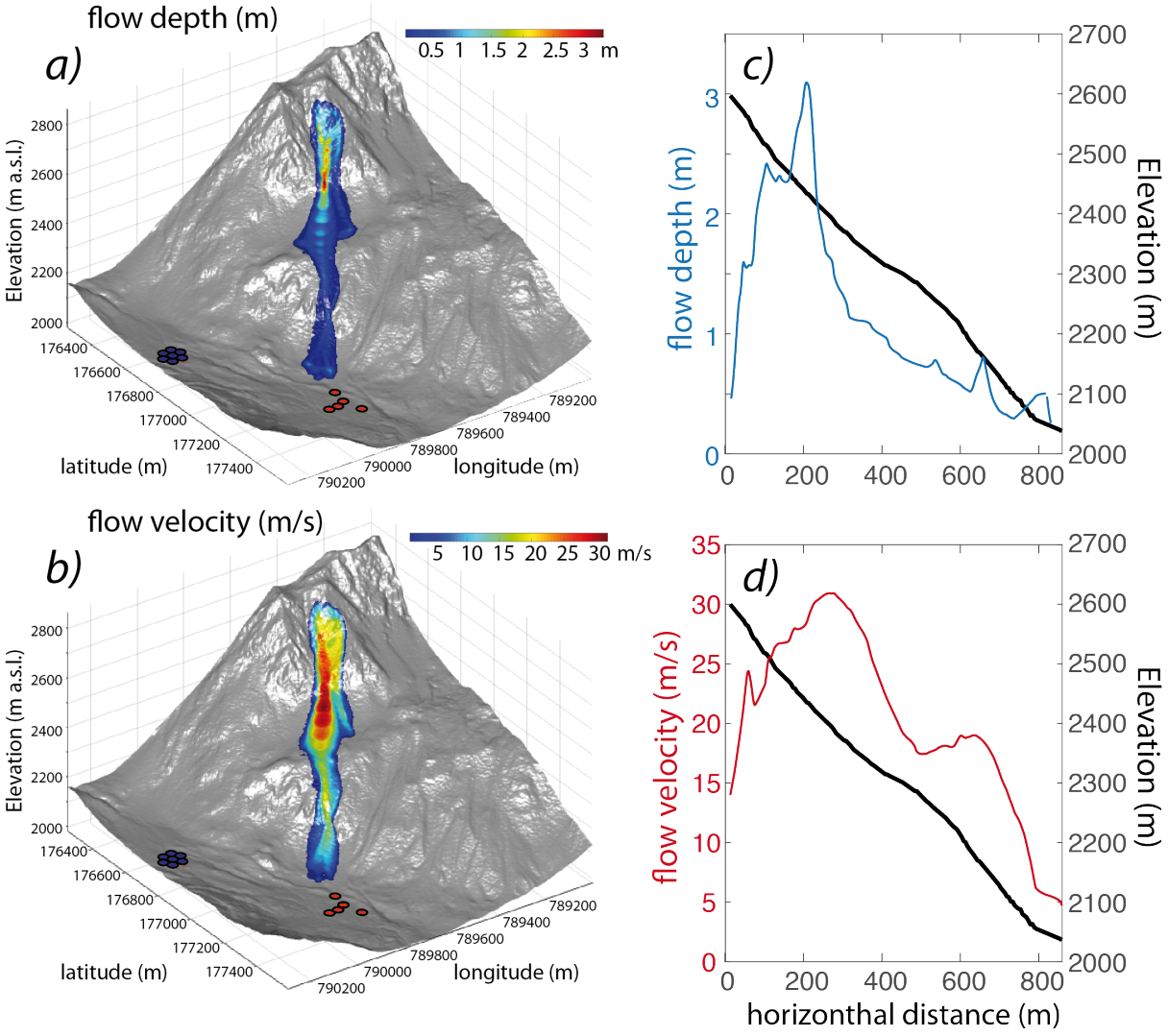


**Figure 8.** Figure showing the flow extent modeled by RAMMS and highlighting maximum flow depth (a) and flow velocity (b). Profiles of the modeled flow depth (c) and flow velocity (d) along the path overimposed on the avalanche path profile (black line) as a function of the travelled horizontal distance.

The flow evolution modeled by RAMMS (Figure 8) appears to be consisted with the two distinct phases observed both for the seismic and infrasound signal. These two phases appear to be controlled by the path geometry forcing the avalanche to slow down and loose mass at the terrain break at an elevation of 2300 m.

## 5 Discussion

The clear variation of the back-azimuth and apparent velocity of the recorded infrasound signals provides a strong constraint on the source mechanism of infrasound energy. The comparison of infrasound radiation area (Figure 7d) with RAMMS modeling (Figure 8), clearly shows that infrasound is radiated when the flow is accelerated within the channel. This is in agreement with the hypothesis that infrasound is produced by the power cloud and with the dynamical evolution of a PSA in terms of an eruption current (*Carrol et al.*, 2013). They showed that the powder cloud formation is strongly enhanced by the narrowing of the avalanche path, while it is limited by the path spreading in the initiation and deposition area. ~~Our seismic and infrasound array observation, clearly shows that while seismic energy is radiated as an elongated source all along the avalanche path, the infrasound signal is radiated mostly from the powder cloud, that develops only within the narrow avalanche channel and is missing in the wider starting and deposition areas~~

## 6 ~~Discussion~~

~~Our results show that seismic and infrasound energies are radiated in different parts of the avalanche path. Seismic energy is radiated all along the path, while infrasound is radiated when the flow is accelerated within the channel. Moreover, the observed trend of back-azimuth suggests that infrasound is likely produced by~~ , in case of multiple sources, the ~~downhill moving powder cloud. The cloud can be approximated~~ array analysis identifies the most energetic source. Therefore, being able to detect and track one predominant source (Figure 6c,e), moving downhill with time, we suggest that snow avalanches are characterized by a dominant source of infrasound energy, allowing to treat the source mechanism of infrasound mostly as a point source moving downhill. This is very different from other density currents, like debris flows, where recorded infrasound is lacking a clear correlation thus limiting the efficiency of array processing procedures (*Marchetti et al.*, 2020). Differently from infrasound, ~~which radiates infrasound from a single position at a given time. Differently ,~~ the scattered back-azimuth of seismic detections (Figure 6d) suggests that seismic signals are most likely produced by multiple sources, or by an elongated source, acting along the path at the same time (Figure 6d,f).

Previous studies (*Surinach et al.*, 2001; *Vilajosana et al.*, 2007b) showed that seismic signals produced by snow avalanches mostly consist of surface waves. They assumed that the seismic energy was radiated mostly by the basal friction and snow ploughing at the avalanche front ~~(*Vilajosana et al.*, 2007b)~~(*Vilajosana et al.*, 2007b, and references therein). The seismic energy was calculated accounting for geometrical spreading and attenuation of surface waves along the front-to receiver distance. Any possible contribution from multiple sources along the path or by an elongated source were not considered. This could lead to an underestimation of the total seismic energy of the event.

An additional constraint to be considered is that the recorded seismic amplitude is possibly increased by the sound transmitted locally into the ground, as suggested already by *Kogelnig et al.* (2011). In this study, this process is confirmed by the combined analysis of seismic and infrasound detections (Figure 6). ~~During the phase of maximum infrasound radiation, the recorded seismic signal is propagating at the velocity of sound (shaded area in Figure 6)~~Considering the apparent velocity of seismic waves, the array processing highlights high values ($>$ 650 m/s) at the beginning and at the end of the event. These values are in agreement with phase velocities (500-950 m/s) measured by *Vilajosana et al.* (2007a) for snow avalanches in Ryggfonn in Norway, as well as values used by *Lacroix et al.* (2012) for beamforming in the French Alps. The central part of the signal, between 05:19:00 and 05:19:15 UT, is characterized by a lower propagation velocity ($\approx$ 330 m/s), suggesting that the seismic array is likely recording infrasound waves. This corresponds to the time when the infrasound amplitude was maximum (Figure 6a). We suggest that the central part of the signal is strongly affected by the infrasound radiated by the event, that converts to seismic waves at the earth free surface and is efficiently recorded by seismometers. This is an agreement with results obtained by *Heck et al.* (2017) for an avalanche that did occur from the same path in 2017, and applying the multiple signal classification (MUSIC) analysis to seismic array data. ~~This indicates that infrasound energy is transmitted locally to the ground and recorded with seismometers. Sound propagation velocities of seismic signals produced by snow avalanches were reported also for previous seismic array investigations (*Heck et al.*, 2017; *Lacroix et al.*, 2012).~~

The process of infrasound to seismic energy transition was described by *Ichihara et al.* (2012). An infrasonic wave hitting the ground ($p(t,x)$) produces a vertical ground velocity ($w(t,x)$) that is directly proportional to the amplitude of the incident wave ($w(t,x) = Hp(t,x)$). The conversion factor ($H$) is defined as:

$$H = \frac{\exp(\frac{-i\pi}{2})c}{2(\lambda+\mu)}\frac{\lambda+2\mu}{\mu}, \tag{1}$$

where $\lambda$ and $\mu$ are Lame's constants of the ground and $c$ is the velocity of sound. It is worth noting how equation (1) is derived for longitudinal waves (pressure wave in the atmosphere and vertical gorund velocity for seismic wave) and it does not account for any frequency dependance. Considering typical values of the Lame's constant for soil ($\approx 10^8$) Pa, and a sound velocity ($c$) of 340 m/s, the conversion factor ($H$) results $\approx 5x10^{-7}$ m/s/Pa. Therefore, an infrasonic wave of 1 Pa will produce a detectable seismic signal in the ground. In the specific case of the 5 February avalanche (Figure 4), the recorded pressure of 0.4 Pa, will produce a seismic signal with an amplitude of $\approx 3x10^{-7}$ m/s, that over-imposes on the body and surface seismic waves produced at the source and corresponds to $\approx 20$ % of the recorded seismic amplitude, in our frequency range ($>$ 4.5 Hz) of analysis. This is in agreement with sound velocities recorded in the seismic data during the phase of maximum infrasound radiation (Figure 6).

This study, combining for the first time seismic and infrasound array data, highlights the complexity of the seismic radiation by snow avalanches and the contribution of the air-to-ground energy transmission. These have an influence on the recorded seismic signal and, if not accounted for, might limit the applicability of seismic signals for energy estimations. The absolute seismic amplitude, and corresponding energy, can change according to snow characteristics (dry/wet) (*Vilajosana et al.*, 2007b), and efficiency of air-to-ground energy transmission (*Ichihara et al.*, 2012). This approach is even more critical considering that

seismic energy is radiated all along the avalanche path (Figure 7a). Moreover, it requires a-priori characterization of the quality factor of surface waves at the site (*Vilajosana et al.*, 2007b), thus preventing a general application of the proposed procedure at various sites.

Similarly, infrasound amplitude is expected to change dramatically as a function of avalanche type (dry/wet) and path geometry, and our results suggest that estimating avalanche size from infrasound signals could be difficult. Signal duration is, for example, reflecting only the part of the path where the avalanche is accelerated, or where the powder cloud develops (Figure 7d). Considering the radiation of sound by a moving body assumed to be a solid sphere, *Naugolnykh and Bedard* (1990) suggested that the frequency of recorded infrasound must scale inversely with the body size as follow:

$$f = c/\pi D, \tag{2}$$

where $c$ is the velocity of sound in the atmosphere while $D$ is the diameter of the sphere.

For the specific case of the avalanche recorded on 5 February 2016, eq 2 predicts a moving sphere-like body with diameter $D$ of $\approx$ 30 m. This value is obtained by assuming a sound propagation velocity of 330 m/s and considering a peak frequency of 3.3 Hz (Figure 4), and is of the same order as the width of the avalanche channel (<50 m). Nevertheless, a snow avalanche is far from being a rigid sphere moving in the atmosphere. Already *Naugolnykh and Bedard* (1990), suggested that additional processes might contribute to the avalanche infrasound radiation, such as the turbulent pressure pulsation of the powder cloud and/or secondary source mechanisms. *Kogelnig et al.* (2011) successfully modeled the pressure amplitude radiated by a snow avalanche at the Vallée de la Sionne test site, considering a moving turbulent source, where pressure amplitude was dependent on flow dimension and velocity, inferred from independent observation of the event. Therefore, while the approach proposed ~~by *Naugolnykh and Bedard* (1990) seems working~~ here following *Naugolnykh and Bedard* (1990) seems to work fine as a first approximation, analyses will be required to further investigate the source mechanisms of infrasound possibly combining infrasound, seismic and high resolution video observation.

## 6 Conclusions

Results presented here, and obtained from seismic and infrasound array analysis for a powder snow avalanches at short ($<$ 1000 m), highlight two separate mechanisms of elastic energy radiation by a snow avalanche. The infrasound energy is radiated only when the powder part develops, and is not produced during the initiation or deposition phase. The duration of the infrasound signal is thus not representative of the entire volume of snow that was transported by the avalanche. Because of the clear migration of infrasound detections in terms of back-azimuth and apparent velocity, we suggest that the source mechanism of the infrasound signal can be interpreted as a moving point source. The clear ~~wave parameters~~ variation of back-azimuth and apparent velocity obtained from the array analysis, suggest that infrasound can be used as an efficient monitoring for avalanche detection purposes in case a powder cloud develops. Back-projection of the infrasound detections on the avalanche path, suggested that the infrasound energy is radiated only when the flow is confined within a narrow path. According to the analytical formulation of *Carrol et al.* (2013), such a condition enhances the formation of the powder front.

The seismic signal is, instead, produced during the entire avalanche evolution, including the initiation and deposition area. Therefore, the signal duration is longer and more representative of the entire flow evolution and run-out distance. Unlike for infrasound, the seismic back-azimuth and apparent velocity values were more scattered, and this makes the detection and location of avalanche events less straightforward than with infrasound. Furthermore, the scattering of wave parameters suggests multiple sources that act simultaneously along the path.

In agreement with *Heck et al.* (2017), the combined seismic and infrasound array analysis, showed also that during the phase of maximum infrasound radiation, seismic energy is strongly affected by the infrasonic signal. In the specific case presented here, where the different frequency response of the infrasound ($> 0.01$ Hz) and seimsic ($> 4.5$) limits the analysis to the high frequency component ($> 4.5$ Hz) of the elastic energy radiation, infrasound contributes to $\approx 20$ % of the recorded seismic amplitude. This needs to be accounted for, when the seismic amplitude is used to estimate the avalanche energy. Similarly, the amplitude of recorded infrasound is controlled by the avalanche type (wet/dry) and the flow evolution (i.e. the formation of the powder cloud). Good results are obtained, for the avalanche event investigated here, considering the frequency of the recorded infrasonic signal, and assuming the source as being produced by a moving sphere (*Naugolnykh and Bedard*, 1990). For the specific case of the avalanche of 5 February 2016, the recorded peak infrasound frequency of 3.3 Hz is consistent with a sphere like body with a diameter of 30 m, in agreement with the the geometry and extension of the avalanche path. Such an approach could be used as a first approximation of the volume involved in case independent observations are available, but can not explain, on its own, the recorded infrasound signal, where a moving turbulent source has been considered to model recorded infrasound at instrumented sites (*Kogelnig et al.*, 2011).

Although many open questions remain concerning the mechanisms of infrasound and seismic energy radiation by snow avalanches, the combined seismic and infrasound array analyses presented in this study helped in clarifying some key aspects of the recorded seismic and infrasound signals, like source origin, possible source mechanisms and mutual relation. Further studies will be required, however, to investigate in detail the source mechanisms of elastic anergy radiation, secondary source processes, like turbulence of the powder front, and possible use of the seismic and the infrasound signal to evaluate the magnitude of the event.

*Data availability.* Infrasound and seismic detections resulting from array processing and used here to achieve most of the findings and create most of the figures are freely available in the Open Science Framework repository (https://osf.io/p28gc/), doi:10.17605/OSF.IO/P28GC.

*Video supplement.* RAMMS::Avalanche simulation, depicting the flow depth (m) along the avalanche path. Red colors indicate flow depths larger than 2m.

*Author contributions.* All of the authors contributed actively to the manuscript. In detail, E.M. and A.H. initiated this study, installed and maintained the instrumentation during the winter season. They worked on the infrasound and seismic data array analysis, developed the model of infrasound and seismic energy partitioning and wrote to the text. M.C. performed the RAMMS modeling of the avalanche. M.C.S. and G.B. contributed to the text, figure and discussion. M.C.S. worked primarily on seismic data while G.B. worked mostly on infrasound data and developed the relationship between infrasound and volume.

*Competing interests.* No competing interests are present.

*Acknowledgements.* Part of this research was supported by a grant of the Swiss National Science Foundation (200021149329).

## References


Adam, V., Chritin, V., Rossi, M., and Van Lancker, E.: Infrasonic monitoring of snow-avalanche activity: what do we know and where do we go from here?, Annals of Glaciology, 26, 324-328, 1998.

Bedard, A.: Detection of avalanches using atmospheric infrasound, Proceedings of the Western Snow Conference, edited by: Shafer, B., Western Snow Conference, April 1989, Colorado State University, Fort Collins, CO, USA, 52–58, 1989.

Biescas, B., F. Dufour, G. Furdada, G. Khazaradze, and E. Suriñach: Frequency content evolution of snow avalanche seismic signals. *Surv. Geophys.* 24, 447–464, 2003.

Carrol, C.S., Louge, M.Y., and Turnbull, B.: Frontal dynamics of powder snow avalanches. *Journ. Geophys. Res. Earth Sur.* 118, 913-924, doi:10.1002/jgrf20068, 2013.

Christen, M., Kowalski, J., and Bartelt, P.: RAMMS: Numerical simulation of dense snow avalanches in three-dimensional terrain. *Cold Reg. Sc. Techonl.* 63, 1-14, doi:10.1016/j.coldregions.2010.04.005, 2010.

Chritin, V., Rossi, M., and Bolognesi, R.: Acoustic detection System for Operational Avalanche Forecasting, Proceeding of International Snow Science Workshop, Banff, Alberta, 6-11 October 1996, 129-133, 1996.

Comey, R.H., and Mendenhall, T.: Recent Studies Using Infrasound Sensors to Remotely Monitor Avalanche Activity. Proceeding of International Snow Science Workshop, Jackson, WY, 19-24 September 2004, 640-646, 2004.

Hammer, C., Fah, D., and Ohrnberger, M.: Automatic detection of wet-snow avalanche seismic signals. *Nat. Hazards* 86, 601-618, doi:10.1007/s11069-016-2707-0, 2017.

Havens, S., Marshall, H.P., Johnson, J.B., and Nicholson, B.: Calculating the velocity of a fast-moving snow avalanche using an infrasound array. *Geophys. Res. Lett.* 41, 6191-6198, doi:10.1002/2014GL061254, 2014.

Heck, H., Hobiger, M., van Herwijnen, A., Schweizer, J., and Fah, D.: Localization of seismic events produced by avalanches using multiple signal classification. *Geophys. J. Int.* 216, 201-217, doi:10.1093/gji/ggy394, 2017.

Ichihara, M., Takeo, M., Yokoo, A., Oikawa, J. and Ohminato, T.: Monitoring volcanic activity using correlation patterns between infrasound and ground motion. *Geophys. Res. Lett.* 39, L04304, doi:10.1029/2011GL050542, 2012.

Issler, D.: Experimental information on the dynamics of dry-snow avalanches, in *Dynamic Response of Granular and Pouros Materials under Large and Catastrophic Deformations, Lecture Notesin Applied and Computational Mechaniscs*, edited by K. Hutter, and N. Kirchner, pp. 109-160, vol. 11, Springer, Berlin, Germany, 2003.

Kishimura, K., and Izumi, K.: Seismic signals induced by snow avalanche flows. *Nat. Hazards* 15(1), 89-100, 1997.

Kogelnig, A., Surinach, E., Vilajosana, I., Hubl, J., Sovilla, B., Hiller, M., and Dufour, F.: On the complementariness of infrasound and seismic sensors for monitoring snow avalanches. *Nat. Hazards Earth Syst. Sci.* 11, 2355-2370, doi:10.5194/nhess-11-2355-2011, 2011.

Kohler, A., McElwaine, J.N., and Sovilla, B.: GEORADAR data and teh flow regimes of snow avalanches. *J. Geoph. Res.: Earth Surface* 123, 1272-1294, doi:10.1002/2017JF004375, 2018.

Lacroix, P., Grasso, J.-R., Roulle, J., Giraud, G., Goetz, D., Morin, S., and Helmstetter, A.: Monitoring of snow avalanches using a seismic array: Location, speed estimation, and relationships to meteorological variables. *J. Geophys. Res.* 117, F01034, doi:10.1029/2011JF002106, 2012.

Louge, M.Y., Turnbull, B., and Carrol, C.S.: Volume growth of a powder snow avalanches. *Annals of Galciology* 53, 57-60, doi:10.3189/2012AoG61A030, 2012.

Marchetti, E., Ripepe, M., Ulivieri, G., and Kogelnig, A.: Infrasound array criteria for automatic detection and front velocity estimation of snow avalanches: towards a real-time early-warning system. *Nat. Hazards Earth. Syst. Sci.* 15, 2545–2555, doi:10.5194/nhess-15-2545-2015, 2015.

Marchetti, E., van Herwijnen, A., Christian, M., Silengo, M. C., and Barfucci, G.: Seismo-acoustic energy partitioning of a powder snow avalanche: data. *Open Science Framework Repository* doi:10.17605/OSF.IO/P28GC, 2020.

Marchetti, E., Walter, F., Barfucci, G., Genco, R., Wenner, M., Ripepe, M., McArdell, B., and Price, C.: Infrasound array analysis of debris flow activity and implication for early warning. *J. Geoph. Res.: Earth Surface* 124, doi:10.1029/2018JF004785, 2019.

Mayer, S., van Herwijnen, A., Ulivieri, G., and Schweizer, J.: Evaluating the performance of operational infrasound avalanche detection systems. *Geop. Res. Abstracts, EGU General Assemply*, 2018.

Naugolnykh, K., and Bedard, A.: ~~Model~~ A model of the avalanche ~~infrasound radiation. Proceeding of International Snow Science Workshop, Jackson, WY, 19-24 September 2004, 871-872, 1990.~~ infrasonic radiation. IEEE International Geoscience and Remote Sensing Symposium DOI: 10.1109/IGARSS.2002.1025713.

Sabot, F., Naaim, M., Granada, F., Surinach, E., Planet-Ladret, P., and Furdada, G.: Study of the avalanche dynamics by means of seismic methods, image processing techniques and numerical models. *Ann. Glaciol.* 26, 319–323, 1998.

Schaerer, P., and Salway, A.: Seismic and impact-pressure monitoring of flowing avalanches. *J. Glaciol.* 26, 179–187, 1980.

Scott, E.D., Hayward, C.T., Kubichek, R.F., Hamann, J.C., Pierre, J.W., Corney, B., and Mendenhall, T.: Single and multiple sensor identification of avalanche-generated infrasound. *Cold Reg. Sci. Technol.* 47, 159-170, 2007.

Steinkogler, W., Sovilla, B., and Lehning, M.: Influence of snow cover properties on avalanche dynamics. *Cold Reg. Sc. Technol.* 97, 121-131, doi:10.1016/j.coldregions.2013.10.002, 2014.

Surinach, E., Furdada, G., Sabot, F., Biescas, B., and Vilaplana, J.M.: On the characterization of seismic signals generated by snow avalanches for monitoring purposes. *Ann. Glaciol.* 32, 268-274, 2001.

Ulivieri, G., Marchetti, E., Ripepe, M., Chiambretti, I., De Rosa, G., and Segor, V.: Monitoring snow avalanches in Northwestern Italian Alps using an infrasound array. *Cold Reg. Sci. Tech.* 69, 177–183, doi:10.1916/j.coldregions.2011.09.006, 2011.

van Herwijnen, A., and Schweizer, J.: Seismic sensor array for monitoring an avalanche start zone: Design, deployment and preliminary results. *J. Glaciol.* 57(202), 267–276, doi:10.3189/002214311796405933, 2011a.

van Herwijnen, A., and Schweizer, J.: Monitoring avalanche activity using a seismic sensor. *Cold Reg. Sc. and Tech.* 69(2-3), 165-176, doi:10.1016/j.coldregions.2011.06.008, 2011b.

Vilajosana, I., Khazaradze, G., Surinach, E., Lied, E., and Kristensen, K.: Snow avalanche speed determination using seismic methods. *Cold Reg. Sci. Tech.* 49, 2–10, doi:10.1016/j.coldregions.2006.09.007, 2007a.

Vilajosana, I., E. Surinach, G. Khazaradze, and Gauer, P.: Snow avalanche energy estimation from seismic signal analysis, *Cold Reg. Sci. Tech.* 50, 72–85, 2007b.